

## Fatigue reliability analysis of welded joints of a TLP tether system

M. Amanullah†, N. A. Siddiqui‡, A. Umar‡ and H. Abbas‡†

*Department of Civil Engineering, Aligarh Muslim University, Aligarh, -202 002, India*

*(Received September 12, 2001, Accepted September 23, 2002)*

**Abstract.** Tethers of Tension Leg Platform (TLP) are a series structural system where fatigue is the principal mode of failure. The present study is devoted to the fatigue and fatigue fracture reliability study of these tethers. For this purpose, two limit state functions have been derived. These limit state functions are based on  $S-N$  curve and fracture mechanics approaches. A detailed methodology for the reliability analysis has then been presented. A sensitivity analysis has been carried out to study the influence of various random variables on tether reliability. The design point, important for probabilistic design, is located on the failure surface. Effect of wind, water depth, service life and number of welded joints are investigated. The effect of uncertainties in various random variables on tether fatigue reliability is highlighted.

**Key words:** series system; fatigue reliability; tension leg platform; offshore structures.

---

### 1. Introduction

Fatigue damage over a period of time is invariably present in any structural system: series or parallel, subjected to alternating loads. It depends upon the number of cycles and stress reversals and the stress amplitude. Tethers of Tension Leg Platforms (TLP) are chain like series structural systems where fatigue is the principal mode of failure (Fig. 1). These tethers of Tension Leg Platforms are highly vulnerable to considerable fatigue damage in their service life. Many investigators [Kjerentroyen and Wirsching (1984), Torng and Wirsching (1991) and Siddiqui and Ahmad (2001)] have investigated the fatigue reliability analysis of these tether systems. TLP tether systems are made up of many tethers connected in series by means of welded joints. The failure of these joints should be studied to assess the fatigue reliability of this system. Two general approaches are reported in the literature for fatigue and fracture reliability analysis of these tethers: (1)  $S-N$  curve approach [Kjerentroyen and Wirsching 1984, Siddiqui and Ahmad (1999)] and (2) Fracture mechanics approach [Torng and Wirsching (1991) and Siddiqui and Ahmad (2001)]. Kjerentroyen and Wirsching (1984) carried out the reliability analysis of TLP tethers assuming them to be a series structural system. Torng and Wirsching (1991) determined the total fatigue life as the summation of initiation life and propagation life, described by characteristic  $S-N$  curves and the Paris law respectively. Siddiqui and Ahmad (1999, 2001) studied the fatigue reliability of TLP tethers under random wave and wind excitations.

---

†M. Tech.

‡Lecturer

‡†Professor

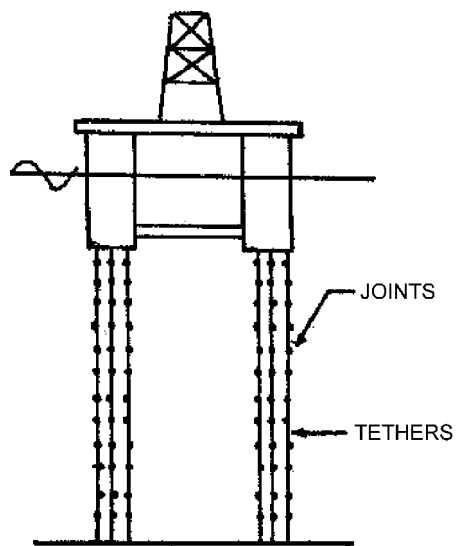


Fig. 1 Tensing leg platform

A detailed review of the past investigations shows that some very important studies such as sensitivity analysis and effect of random wind were not included in the reliability assessment of tether system. The present study is devoted to the fatigue and fatigue fracture reliability study of these tethers. For this purpose, limit state functions have been derived that are based on  $S-N$  curve and fracture mechanics approaches. A detailed methodology for the reliability analysis has then been presented. To study the influence of various random variables on tether reliability sensitivity analysis have been carried out. The design point, important for probabilistic design, is located on the failure surface. The effect of wind, water depth, service life and number of welded joints are investigated. The effect of uncertainties in various random variables on tether fatigue reliability is highlighted.

## 2. Fatigue reliability formulation

Fatigue reliability analysis has been carried out under the following assumptions and idealizations:

- 1) The elements of tethers are joined together to make a complete tether by means of welding and thus forming a series system.
- 2) System failure has been defined as the failure of one of the tethers in one of the legs of TLP.
- 3) There is no correlation among tether joints.
- 4) There is no inspection or repair programme of TLP joints before failure.

### 2.1. Limit state function

A limit state function is a prerequisite for the fatigue reliability analysis. Based on the above assumptions and idealizations following two models have been employed to formulate the limit state functions for fatigue reliability analysis:

- *S-N* curve model; and
- Fracture mechanics model.

2.1.1. *S-N* curve model

In this approach, the fatigue strength is expressed through the *S-N* relation which gives the number of stress cycles *N* with stress range *S* to cause failure. The *S-N* model generally used for high-cycle fatigue is given as

$$NS^m = A \tag{1}$$

where *S* is the stress range; *m*, *A* are empirical constants; and *N* is the number of cycles to cause failure.

The TLP is subjected to environmental loadings, random in nature. Consequently the stress process is a stochastic process and each stress range is a random variable. The fatigue damage under stochastic loading has been estimated by the Miner-Palmgren model. Using this model we get the total accumulated damage *D* in lifetime of the structure *T<sub>s</sub>* as (Siddiqui and Ahmad 2001).

$$D = \sum_{j=1}^{N(T_s)} \frac{S_j^m}{A} \tag{2}$$

where *N(T<sub>s</sub>)* is the total number of stress cycles in time *T<sub>s</sub>*. In this formulation it is assumed that the accumulated damage *D* is independent of the sequence in which stress cycles occur. Since each

stress range is a random variable  $\sum_{j=1}^{N(T_s)} S_j^m$  is also a random variable. If *N(T<sub>s</sub>)* is sufficiently large, the uncertainty in the sum is very small and the sum can be replaced by its expected value. Therefore,

$$E \left[ \sum_{j=1}^{N(T_s)} S_j^m \right] = E[N(T_s)]E[S_j^m] \tag{3}$$

For a narrow-band Gaussian process, stress ranges are Rayleigh-distributed. The mean value of the stress range follows directly as

$$\begin{aligned} E[S_j^m] &= \int_0^\infty (2q)^m \frac{q}{\sigma_q} \exp\left(-\frac{1}{2}\left(\frac{q}{\sigma_q}\right)^2\right) dq \\ &= (2\sqrt{2})^m \sigma_q^m \Gamma\left(1 + \frac{m}{2}\right) \end{aligned} \tag{4}$$

Then, the accumulated damage *D* is written as

$$D = \frac{1}{A} E[N(T_s)]E[S^m] \tag{5}$$

If we consider the environmental condition being described as a set of stationary short-term sea

states, the total damage can be obtained by summing the accumulated damage over all the sea states. Thus, the total damage  $D$  using Eqs. (4) and (5) for all the sea states yields:

$$D = \frac{T_s}{A} \Omega \quad (6)$$

where  $\Omega$  is a stress parameter and it is given by

$$\Omega = (2\sqrt{2})^m \Gamma\left(1 + \frac{m}{2}\right) \sum_{q=1}^n f_q v_{0q} \sigma_q^m \quad (7)$$

where

$v_{0q}$  = mean zero crossing frequency of random stress process in  $q$ th sea state

$f_q$  = fraction of time in  $q$ th sea state

$\sigma_q$  = R.M.S. of stress process in  $q$ th sea state

In above expression  $T_s$  is years in service,  $v_{0q} = \frac{1}{2\pi} \sqrt{\frac{m_2}{m_0}}$ , is zero crossing frequency of the stress process in  $q$ th sea state,  $\sigma_q = \sqrt{m_0}$ , is R.M.S value of the stress process in  $q$ th sea state.  $m_n = \int_0^\infty \omega^n S(\omega) d\omega$  is  $n$ th moment of the stress spectrum and  $f_q$  is fraction of the time spent in the  $q$ th sea state (to account for long term sea effect).

Failure will occur if  $D > \Delta_F$  where  $\Delta_F$  is the value of the Miner-Palmgren damage index at failure. Often  $\Delta_F$  is taken as 1.

Letting  $D > \Delta_F$ , the time to fatigue failure  $T$  of a joint using Eq. (6) is obtained as:

$$T = \frac{\Delta_F A}{\Omega} \quad (8)$$

in order to take into account the uncertainties associated with the above expression, the factors involved in the expression shall be modeled as random variables. The time required for failure  $T_i$  of a joint  $i$  is written as

$$T_i = \frac{\Delta_F A}{B^m \Omega} \quad (9)$$

where,  $\Delta_F$ ,  $A$ ,  $B$  = random variables. Here,  $B$  describes the inaccuracies in estimating the fatigue stresses. The actual stress range is assumed to be equal to the product of  $B$  and the estimated stress range  $S_i$ . The uncertainties in fatigue strength, as evidenced by scatter in  $S-N$  data, are accounted for by considering  $A$  to be a random variable. The random variable  $\Delta_F$  quantifies modeling error associated with the Miner-Palmgren rule.

The fatigue failure occurs when the random variable  $T_i$  is smaller than  $T_s$  where  $T_s$  is the lifetime of the structure. Thus, the limit state function is

$$Z(\underline{X}) = \frac{\Delta_F A}{B^m \Omega} - T_s \quad (10)$$

$$\text{where, } \underline{X} = (\Delta_F, A, B) \quad (11)$$

and thus probability of failure,  $P_f$  can be defined as

$$P_f = P(T_i \leq T_s) = P[Z(\underline{X}) \leq 0] \quad (12)$$

The above failure probability is computed using First Order Reliability Method (FORM, Madsen *et al.* 1986).

The reliability or safety index is thus obtained by

$$\beta = \Phi^{-1}(P_f) \quad (13)$$

where  $\beta$  is a Hasofer-Lind reliability index;  $\Phi^{-1}()$  is the inverse of the standardized normal distribution function.

### 2.1.2. Fracture mechanics model

In the present study Linear elastic fracture mechanics has been adopted for limit state function formulation. In this approach, relationships between average increment in crack growth ( $da/dN$ ) during a load cycle and a global parameter are developed. The most popular global parameter used is the stress-intensity factor,  $K$ , which gives the magnitude of the stresses in the crack-tip region as a function of type and magnitude of loading and geometry of the cracked body.  $K$  is usually expressed as:

$$K = Y(a)S\sqrt{\pi a} \quad (14)$$

where

$a$  = crack size;

$S$  = far-field stress due to applied load; and

$Y(a)$  = geometry function which takes into account crack geometry and specimen shape.

In the present study an empirical expression given by Kung and Wirsching (1992) for welded joints has been used. This expression for  $Y(a)$  is

$$Y(a) = 1.0 a^{-0.125} \quad (15)$$

Many crack growth relationships are available in the literature. The following expression developed by Paris (1964) is one of the most in use relation for predicting the rate of crack growth ( $da/dN$ ):

$$\frac{da}{dN} = C(\Delta K)^m \quad (16)$$

$$\text{where } \Delta K = Y(a)\Delta S\sqrt{\pi a} \quad (17)$$

in which  $\Delta K$  is the stress-intensity factor range in a stress cycle and  $C$  and  $m$  are material constants.

Substituting the expression for  $\Delta K$  into Eq. (16) and integrating over  $da$  and  $dN$ , the following relation between crack size  $a$  and number of stress cycles  $N$  in time  $T_s$  is obtained:

$$\frac{1}{C} \int_{a_0}^a \frac{dz}{Y(z)^m (\sqrt{\pi z})^m} = N(T_s) E(\Delta S^m) \quad (18)$$

This equation has been derived considering variable-amplitude loading. As described in the previous section, the sum of values of stress range in each cycle ( $\sum_{j=1}^{N(T_s)} \Delta S_j$ ) has been approximated by  $N(T_s) E(DS^m)$ . This approximation neglects the effects of load cycle sequence. Assuming the various sea states as a long-term sea states, and the stress range following a Rayleigh distribution in each sea state, we obtain

$$\frac{1}{C} \int_{a_0}^a \frac{dz}{Y(z)^m (\sqrt{\pi z})^m} = T_s \Omega \quad (19)$$

where  $\Omega$  is a stress parameter and it is given by Eq. (7). The failure criteria can then be formulated as a function of crack size. Failure occurs when the crack size exceeds a critical value  $a_c$  which can be based on a serviceability condition. The probabilistic model for the time to failure  $T_i$  of joint  $i$  can be defined as under. It takes into account the uncertainties involved in the fracture mechanics approach in the present model under consideration:

$$T_i = \frac{1}{CB_i^m \Omega_i^m} \int_{a_{0i}}^{a_i} \frac{dz}{\gamma_i Y(z)^m (\sqrt{\pi z})^m} \quad (20)$$

where,  $C$ ,  $B$ ,  $a_{0i}$ ,  $\gamma_i$  are the random variables. Here,  $B$  and  $\gamma_i$  were introduced to model errors in the estimation of the stress range  $\Delta S$  and in the geometry function  $Y(a)$ , respectively.

The fatigue failure occurs when the random variable  $T_i$  is smaller than  $T_s$  where  $T_s$  is the lifetime of the structure. Thus the limit state function is

$$Z(\underline{X}) = \frac{1}{CB^m \Omega^m} \int_{a_{0i}}^{a_i} \frac{dz}{\gamma_i Y(z)^m (\sqrt{\pi z})^m} - T_s \quad (21)$$

$$\underline{X} = (C, B, a_{0i}, \gamma_i) \quad (22)$$

## 2.2. System reliability

A complete tether is formed by number of tether elements connected by welded joints one after the other and thus forms a series or weakest-link system. In the present study all the tether joints are welded and assumed to be mutually independent (i.e., no correlation). The probability of failure of all these joints are the same. However, in some situation the joints near the hull and that near foundation templates may have different probabilities of failure than rest of the other joints. This is due to different stress magnitude near these ends than rest of the joints. The system probability of failure ( $P_{f_{\text{sys}}}$ ) could be estimated in terms of component joints failure probabilities ( $P_{fi}$ ) as given below.

$$P_{f_{sys}} = 1 - \prod_{i=1}^n (1 - P_{fi}) \tag{23}$$

Above equation gives an upper bound on system probability of failure (Kjerengtroen and Wirsching 1984). The above basic equation has been derived under the assumption that events of failure of each member in a series system were mutually independent.

If all the joints (i.e.,  $n$  joints) have the same probability of failure then from Eq. (23) we have

$$P_{f_{sys}} = 1 - (1 - P_{fi})^n \tag{24}$$

Using binomial expansion we have

$$\approx 1 - (1 - nP_{fi} + \dots\dots\dots) \tag{25}$$

since  $P_{fi}$  is significantly small therefore neglecting the higher order terms we get

$$P_{f_{sys}} \approx nP_{fi} \tag{26}$$

Hence, Eq. (26) shows that the system probability of failure is almost directly proportional to the number of tether joints  $n$ .

### 3. Numerical study

For the numerical study, a TLP as shown in Fig. 1 is chosen for the reliability study. Its specifications are given in Table 1 that have been taken from Siddiqui and Ahmad (2000). For reliability analysis we need the response statistics of tether stresses arising due to the action of oscillating random waves. For

Table 1 TLP Description (Siddiqui and Ahmad 2000)

|                                          |                                         |
|------------------------------------------|-----------------------------------------|
| Platform height                          | 80.3 m                                  |
| Total Pretension                         | $1.220 \times 10^8$ N                   |
| Draft                                    | 26.60 m                                 |
| Corner column diameter                   | 14.20 m                                 |
| Center to center column spacing          | 58.30 m                                 |
| Pontoon length                           | 58.30 m                                 |
| Pontoon Diameter                         | 11.00 m                                 |
| Center of gravity above the base line    | 35.85 m                                 |
| Tether length                            | 473.4 m                                 |
| Length of the each element of the tether | 9.75 m                                  |
| Thickness of tether pipe                 | 3.34 cm                                 |
| Youngs modules of tether material        | $2.019 \times 10^{11}$ N/m <sup>2</sup> |
| Number of columns                        | 4                                       |
| Number of joints/tether                  | 50                                      |
| Service life                             | 20 years                                |

Table 2 Statistics of tether stresses (Siddiqui and Ahmad 2001)

| Sea State | Significant wave height $H_s$ (m) | Zero crossing period $T_z$ (sec) | Fraction of time in each sea state | RMS stress (MPa) | Zero crossings Frequency $\nu_{oq}$ (Hz) |
|-----------|-----------------------------------|----------------------------------|------------------------------------|------------------|------------------------------------------|
| S1        | 17.15                             | 13.26                            | 0.00000037                         | 28.21            | 0.072                                    |
| S2        | 15.65                             | 12.66                            | 0.00000238                         | 20.99            | 0.119                                    |
| S3        | 14.15                             | 12.04                            | 0.00001437                         | 15.29            | 0.155                                    |
| S4        | 12.65                             | 11.39                            | 0.00007980                         | 13.04            | 0.204                                    |
| S5        | 11.15                             | 10.69                            | 0.00040572                         | 11.11            | 0.210                                    |
| S6        | 9.65                              | 9.94                             | 0.00187129                         | 10.43            | 0.259                                    |
| S7        | 8.15                              | 9.14                             | 0.00773824                         | 7.71             | 0.217                                    |
| S8        | 6.65                              | 8.26                             | 0.02822122                         | 6.64             | 0.228                                    |
| S9        | 5.15                              | 7.26                             | 0.08851105                         | 5.25             | 0.253                                    |
| S10       | 3.65                              | 6.12                             | 0.22831162                         | 3.12             | 0.260                                    |
| S11       | 2.15                              | 4.69                             | 0.43542358                         | 2.74             | 0.435                                    |
| S12       | 0.65                              | 2.58                             | 0.20942036                         | 1.47             | 0.508                                    |

Table 3 data for reliability study ( $S-N$  model)

| Variable                                           | Distribution | Mean/Median                           | COV  |
|----------------------------------------------------|--------------|---------------------------------------|------|
| Fatigue strength coefficient, $A$                  | Lognormal    | $\tilde{A} = 5.27 \times 10^{12}$ Mpa | 0.63 |
| Stress modeling error, $B$                         | Lognormal    | $\tilde{B} = 1.00$                    | 0.20 |
| Miner-Palmgren damage index at failure, $\Delta_F$ | Lognormal    | $\tilde{D}_F = 1.00$                  | 0.30 |
| Fatigue exponent, $m$                              | Constant     | 3.0                                   |      |

$\sim$  = Median value

$\mu$  = Mean value

COV = Coefficient of variation

Table 4 Data for reliability study (Fracture Mechanics model)

| Variable                            | Distribution | Mean/Median                           | COV  |
|-------------------------------------|--------------|---------------------------------------|------|
| Paris Coefficient, $C$              | Lognormal    | $\tilde{C} = 0.7 \times 10^{-12}$ MPa | 0.63 |
| Stress modeling error, $B$          | Lognormal    | $\tilde{B} = 1.00$                    | 0.20 |
| Initial crack length, $a_0$ (mm)    | Exponential  | $\mu_{a_0} = 0.005$                   |      |
| Modeling error in $Y(a)$ , $\gamma$ | Lognormal    | $\mu_\gamma = 1.00$                   | 0.10 |
| Critical crack length, $a_c$ (mm)   | Constant     | 33.4                                  |      |
| Paris exponent, $m$                 | Constant     | 3.0                                   |      |

$\sim$  = Median value

$\mu$  = Mean value

COV = Coefficient of variation

the present reliability study these statistics, as shown in Table 2, are taken from Siddiqui and Ahmad (2001) for twelve sea states.

Table 5 Tether joint & system  $P_f$  &  $\beta$

|        | S-N model              |         | Fracture mechanics model |         |
|--------|------------------------|---------|--------------------------|---------|
|        | $P_f$                  | $\beta$ | $P_f$                    | $\beta$ |
| Joint  | $2.21 \times 10^{-04}$ | 3.513   | $3.96 \times 10^{-05}$   | 3.947   |
| System | $1.10 \times 10^{-02}$ | 2.290   | $1.98 \times 10^{-03}$   | 2.881   |

### 3.1. Random variables

The random variables considered in the reliability study for S-N model are fatigue strength coefficient (A), stress modeling error (B) and Miner-Palmgren damage index at failure ( $\Delta_F$ ). In fracture mechanics approach, Paris Coefficient (C), stress modeling error (B), initial crack length ( $a_0$ ) and uncertainty factor ( $\gamma$ ) are considered as random variables. A brief description of these variables is summarized in Tables 3 and 4. These values have been taken from Kung and Wirsching (1992).

## 4. Discussion of results

The probabilities of failure and reliability indices of tether joint and system obtained from S-N model and fracture mechanics model under random wave excitation are shown in Table 5.

A comparison of the results obtained from the two models (S-N curve and fracture mechanics) shows that the S-N curve approach gives more conservative results for joint and system reliability. This is due to the reason that the crack initiation is the failure criteria in S-N curve approach while in fracture mechanics approach failure occurs when a crack reaches a certain critical value. In other words in S-N curve approach crack initiation time is compared with service life whereas in fracture mechanics approach crack propagation time to reach a critical crack size is compared with service or design life. Moreover, for tethers it is not realistic to assume the immediate failure as any minor crack appears in

Table 6 Design point values for S-N model

| Random variables | $\Delta_F$ | A                        | B    |
|------------------|------------|--------------------------|------|
| Design values    | 0.71       | $1.4 \times 10^{12}$ MPa | 1.60 |

$\Delta_F$  = Miner-Palmgren damage index at failure

A = Fatigue strength coefficient

B = Stress modeling error

Table 7 Design point values for Fracture mechanics model

| Random variables | C                        | B    | $a_0$     | $\gamma$ |
|------------------|--------------------------|------|-----------|----------|
| Design values    | $1.7 \times 10^{12}$ MPa | 1.36 | 0.0366 mm | 1.08     |

C = Paris coefficient

B = Stress modeling error

$a_0$  = Initial crack length

$\gamma$  = Uncertainty factor in geometric function

the tether joint. The Table also shows that tether system reliability is significantly less than its joint reliability. This is due to the fact that a complete tether forms a series or weakest-link system, for which every addition of joint decreases the system reliability.

#### 4.1. Design point or most probable point

A point on the failure surface that corresponds to the shortest distance from the origin in the reduced coordinate system is defined as the most likely failure point or design point. Tables 6 and 7 show the values of the most likely failure point or design point on failure surface for *S-N* curve and fracture mechanics approaches.

These values of different random variables are essential for reliability-based probabilistic design of tethers. In such designs partial safety factors for load and resistance variables are determined for the target reliability (i.e., target reliability index). The value of the target reliability index which is generally recommended for offshore structural components is 3.00 (Wirsching and Chen 1987). However, the final decision for this value is to be taken by design engineers and professionals. Having decided the target reliability index value, these safety factors are separately defined for resistance and load variables. For resistance variables it is defined as the nominal, mean or characteristic value divided by the design value and for load variables as the design value divided by the nominal, mean or characteristic values.

#### 4.2. Sensitivity analysis

This analysis has been carried out to study the influence of various random variables on tether reliability. The influence of various random variables on tether reliability is measured in terms of sensitivity factor ( $\alpha_j$ ) which for the *j*th random variable is defined as

$$\alpha_j = \frac{\left(\frac{\partial Z_1}{\partial y_j}\right)^*}{\left[\sum_{j=1}^n \left(\frac{\partial Z_1}{\partial y_j}\right)^{2*}\right]^{1/2}} \quad (27)$$

where  $Z_1$  and  $y_j$  indicate the limit state function and *j*th random variable in reduced coordinate system; and \* indicate the most probable or design point on the failure surface.

The above defined sensitivity factors have following characteristics:

1. The lower the magnitude of  $\alpha_j$ , less is the influence of *j*th random variable on the reliability.
2.  $\alpha_j$  is positive for load variables and negative for resistance variables.
3. If  $\alpha_1, \alpha_2, \alpha_3, \dots, \alpha_n$  are the sensitivity factors for *n* random variables appearing in the limit state

function then  $\sum_{j=1}^n \alpha_j^2 = 1$

In the present study, using above expression, sensitivity factors for each random variable have been determined. As mentioned above, the magnitude of this factor for a random variable is directly measure of its influence on tether reliability. However, its sign determines whether the

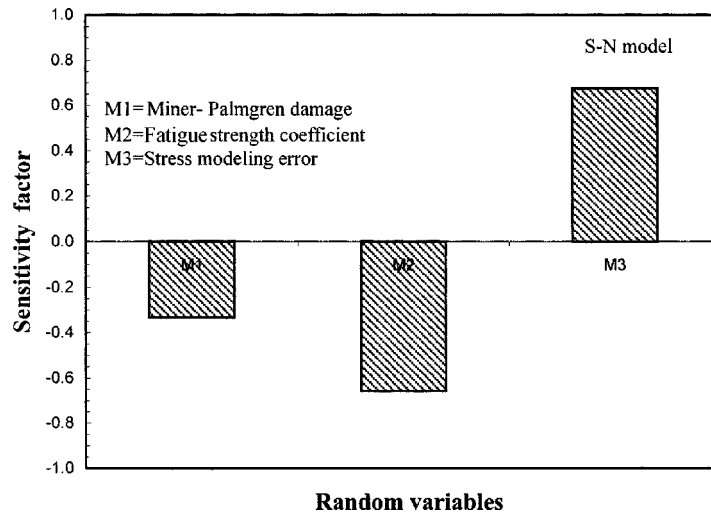


Fig. 2 Sensitivity diagram

random variable is a load variable or resistance variable. The positive value of sensitivity factor indicates that the random variable is a resistance variable i.e., its increase will improve the tether reliability and decrease will reduce the reliability. Similarly negative value of sensitivity factor indicates that it is a load variable and its influence would be opposite to that of a resistance variable. The major advantage of this study is that without carrying out any separate parametric study for each variable one can directly know how a particular random variable affects the tether reliability.

Fig. 2 shows results of sensitivity analysis for *S-N* curve based model. The bar chart indicates that the sensitivity factors for Miner-Palmgren damage index ( $\Delta_F$ ), and fatigue strength coefficient ( $A$ ) are negative hence they are resistance variables and contribute to the resistance part of the limit state function. Sensitivity factor for stress modeling error or response uncertainty factor ( $B$ ), however, is positive thus it will contribute to load part of the limit state function. Therefore, for the given uncertainty, an increase in the magnitude of Miner-Palmgren damage index ( $\Delta_F$ ) and fatigue strength coefficient ( $A$ ) will improve the reliability of tethers, whereas, increase in response uncertainty factor ( $B$ ) will reduce the reliability of TLP tethers. Moreover, the chart shows that out of the two resistance variables, reliability is more sensitive to fatigue strength coefficient ( $A$ ) than Miner-Palmgren damage index ( $\Delta_F$ ).

Fig. 3 shows results of sensitivity analysis for fracture mechanics based model. Sensitivity factors for all these random variables i.e., Paris coefficient ( $C$ ), stress modeling error ( $B$ ), initial crack length ( $a_0$ ), and modeling error in geometry function ( $\gamma$ ) are positive which shows that these variables will contribute to the load part only. This is due to the fact that resistance parameter in this problem is a critical crack size ( $a_c$ ) which has been considered equal to the tether thickness and assumed as deterministic. Since all the random variables are load variables therefore their increase in magnitude for a given uncertainty will decrease the reliability of tethers. Moreover, reliability is most sensitive and least sensitive to initial crack length ( $a_0$ ) and modeling error in geometry function ( $\gamma$ ) respectively. This is due to the highest and lowest magnitude of sensitivity factor for initial crack length ( $a_0$ ) and modeling error in geometry function respectively.

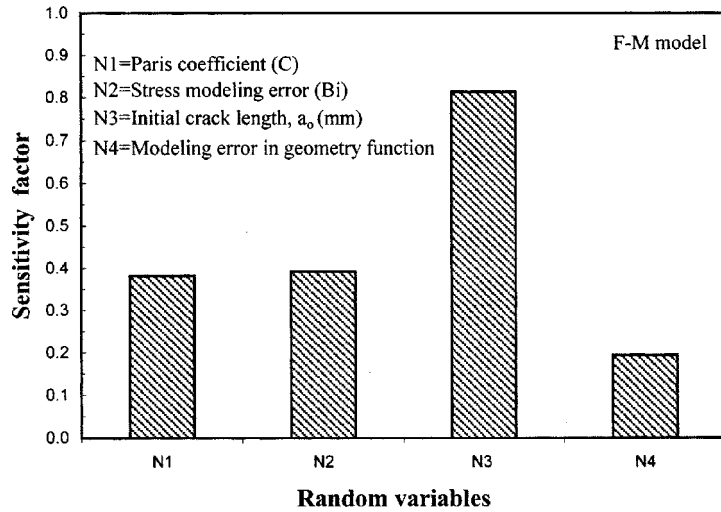


Fig. 3 Sensitivity diagram

### 4.3. Effect of wind

Since wind is the major source of sea wave generation, hence, consideration of wave alone in an open sea environment is not a realistic proposition. To study the effect of wind on reliability we need the response statistics of tether stresses arising due to the action of oscillating random waves and wind. For this purpose again the response statistics have been taken from Siddiqui and Ahmad (2001) for the same twelve sea states, but with the inclusion of wind (Table 8).

Tables 9 and 10 shows the effect of wind on tether reliability and probability of failure. The results show that the inclusion of mean and fluctuating wind causes a reduction of probability of failure by

Table 8 Statistics of tether stresses (Siddiqui and Ahmad 2001)

| Sea State | Significant wave height $H_s$ (m) | Zero crossing period $T_z$ (sec) | Wind velocity $u$ (m/s) | RMS stress $\sigma_q$ (MPa) | Fraction of time in each sea state | Zero crossings Frequency $\nu_{oq}$ (Hz) |
|-----------|-----------------------------------|----------------------------------|-------------------------|-----------------------------|------------------------------------|------------------------------------------|
| S1        | 17.15                             | 13.26                            | 24.38                   | 25.17                       | 0.00000037                         | 0.103                                    |
| S2        | 15.65                             | 12.66                            | 23.29                   | 37.16                       | 0.00000238                         | 0.115                                    |
| S3        | 14.15                             | 12.04                            | 22.15                   | 24.38                       | 0.00001437                         | 0.122                                    |
| S4        | 12.65                             | 11.39                            | 20.94                   | 20.40                       | 0.00007980                         | 0.152                                    |
| S5        | 11.15                             | 10.69                            | 19.66                   | 11.63                       | 0.00040572                         | 0.213                                    |
| S6        | 9.65                              | 9.94                             | 18.29                   | 9.52                        | 0.00187129                         | 0.257                                    |
| S7        | 8.15                              | 9.14                             | 16.81                   | 7.71                        | 0.00773824                         | 0.217                                    |
| S8        | 6.65                              | 8.26                             | 15.18                   | 5.92                        | 0.02822122                         | 0.214                                    |
| S9        | 5.15                              | 7.26                             | 13.36                   | 4.70                        | 0.08851105                         | 0.231                                    |
| S10       | 3.65                              | 6.12                             | 11.25                   | 2.82                        | 0.22831162                         | 0.282                                    |
| S11       | 2.15                              | 4.69                             | 8.63                    | 2.38                        | 0.43542358                         | 0.433                                    |
| S12       | 0.65                              | 2.58                             | 4.75                    | 1.07                        | 0.20942036                         | 0.495                                    |

Table 9 Tether joint & system,  $P_f$  &  $\beta$ , for wave only

|        | S-N model              |         | Fracture mechanics model |         |
|--------|------------------------|---------|--------------------------|---------|
|        | $P_f$                  | $\beta$ | $P_f$                    | $\beta$ |
| Joint  | $2.21 \times 10^{-04}$ | 3.513   | $3.96 \times 10^{-05}$   | 3.947   |
| System | $1.10 \times 10^{-02}$ | 2.290   | $1.98 \times 10^{-03}$   | 2.881   |

Table 10 Tether joint & system  $P_f$  &  $\beta$ , for wave with wind

|        | S-N model              |         | Fracture mechanics model |         |
|--------|------------------------|---------|--------------------------|---------|
|        | $P_f$                  | $\beta$ | $P_f$                    | $\beta$ |
| Joint  | $4.69 \times 10^{-05}$ | 3.906   | $7.93 \times 10^{-06}$   | 4.316   |
| System | $2.34 \times 10^{-03}$ | 2.828   | $3.96 \times 10^{-04}$   | 3.355   |

order one in the tether joint and system. It is mainly due to the attenuating effect of the wind which acts on the exposed superstructure of the TLP. Due to this attenuation effect, reliability index has been improved from 3.513 to 3.906 for S-N model and from 3.947 to 4.316 for fracture mechanics model. Corresponding system reliability has also been improved from 2.290 to 2.828 for S-N model and from 2.881 to 3.355 for fracture mechanics model.

#### 4.4. Effect of service life

Service life or design life directly affects the probability of failure or reliability of a joint and system. Figs. 4 and 5 show that as the service life requirement increases, corresponding reliability sharply decreases. This is an expected trend.

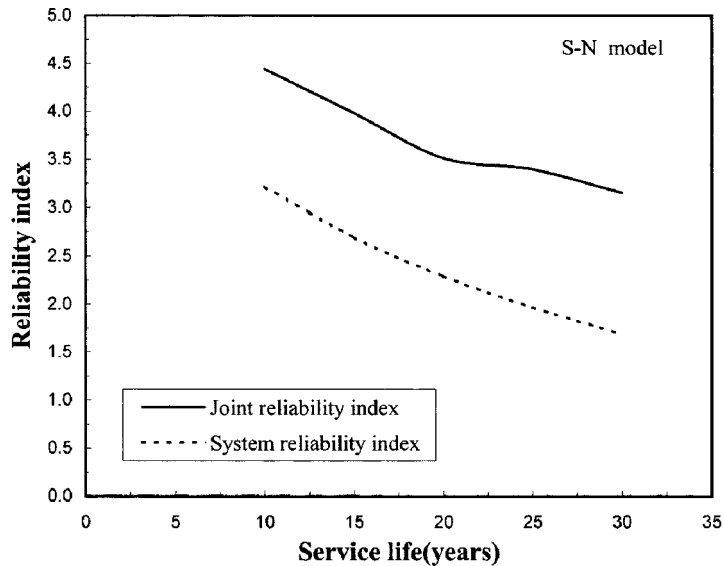


Fig. 4 Effect of service life on reliability

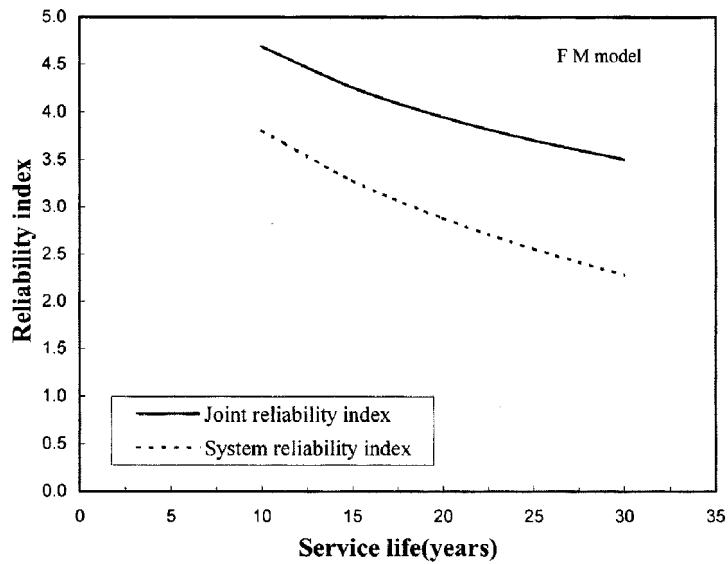


Fig. 5 Effect of service life on reliability

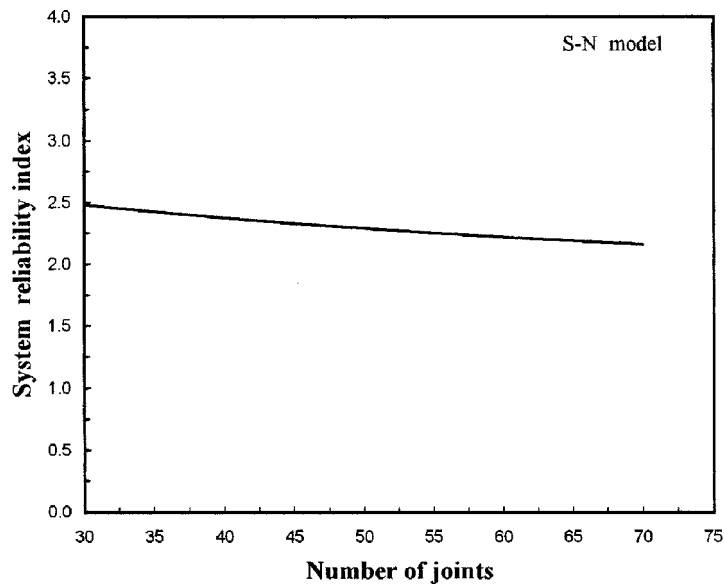


Fig. 6 Effect of number of joints on system reliability

#### 4.5. Effect of number of joints

Figs. 6 and 7 indicate that in a tether system as the number of joints increases reliability decreases. This is because as the number of joints increases the number of weaker locations in the tether system also increases. A single joint consists of only one vulnerable location while these locations increase

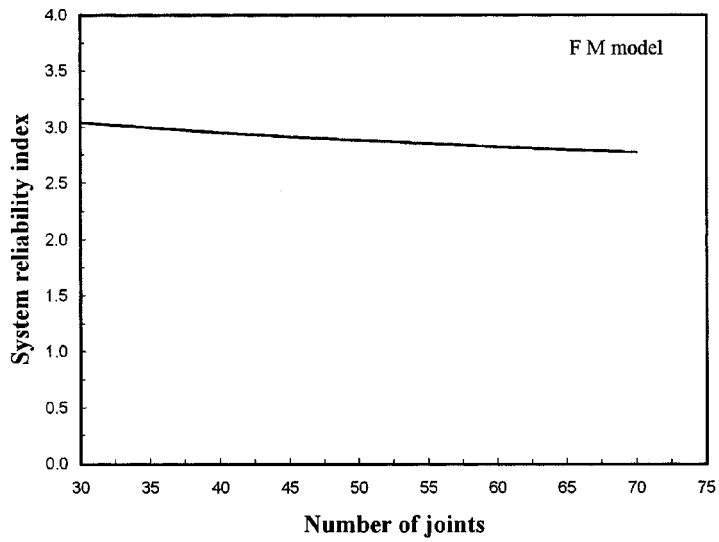


Fig. 7 Effect of number of joints on system reliability

with every addition of tether element. In the present study the reliability index of tether system is about 30% less than that of a joint. Hence for a fixed length of tether element, the reliability of tether system will keep on decreasing with increase in water depth

4.6. Effect of probability distribution

To study the effect of probability distribution on tether reliability; two cases have been considered. In the first case, the actual probability distribution for various random variables have been considered and in the second case all variables are assumed as normally distributed (Tables 11 and 12). If all the random variables are assumed as normally distributed (with the same expected value and variance as the original) the results show that for *S-N* model, the reliability is underestimated, however for fracture mechanics model, it is overestimated. Further, the difference in the reliability magnitudes is also quite considerable.

Table 11 Effect of probability distribution (*S-N* model)

| Sea idealization | Normal distribution   |         | Original distribution  |         |
|------------------|-----------------------|---------|------------------------|---------|
|                  | $P_f$                 | $\beta$ | $P_f$                  | $\beta$ |
| Wave only        | $5.6 \times 10^{-02}$ | 1.513   | $2.21 \times 10^{-04}$ | 3.513   |
| Wave with wind   | $3.6 \times 10^{-02}$ | 1.535   | $4.69 \times 10^{-05}$ | 3.906   |

Table 12 Effect of probability distribution (Fracture mechanics model)

| Sea idealization | Normal distribution    |         | Original distribution  |         |
|------------------|------------------------|---------|------------------------|---------|
|                  | $P_f$                  | $\beta$ | $P_f$                  | $\beta$ |
| Wave only        | $2.04 \times 10^{-06}$ | 4.861   | $3.96 \times 10^{-05}$ | 3.947   |
| Wave with wind   | $2.51 \times 10^{-09}$ | 5.708   | $7.93 \times 10^{-06}$ | 4.316   |

Thus it may be concluded that for fatigue reliability analysis, the normal distribution assumption usually made for many engineering structural reliability analysis, is not an appropriate proposition. This conclusion is valid for both the sea idealization cases: (a) wave only; and (b) wave with wind.

4.7. Effect of variables in S-N model

Figs. 8-11 show effect of various random variables on tether joint and system reliability for given uncertainties. Figs. 8 and 9 show that as the value of fatigue strength coefficient ( $A$ ) and Miner-Palmgren damage index ( $\Delta_F$ ) increases, reliability also increases, however, the rate of increase is more

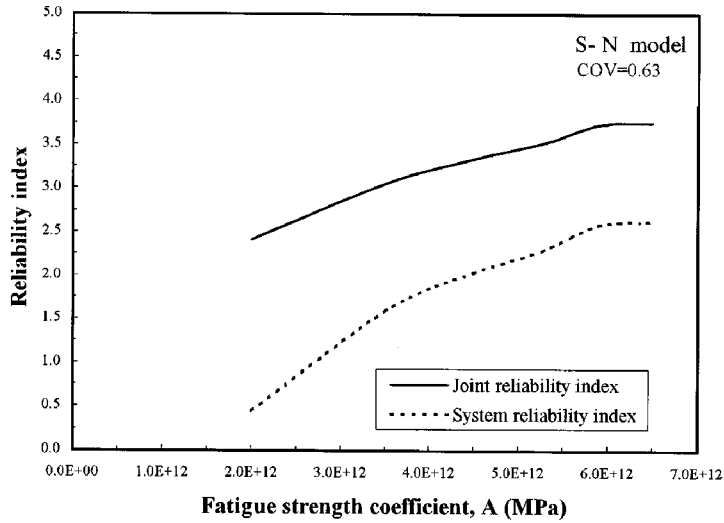


Fig. 8 Effect of fatigue strength coefficient, A (MPa) on reliability

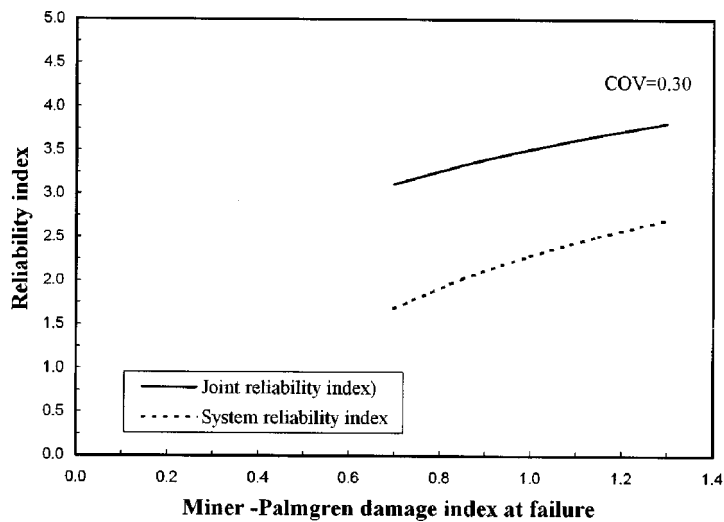


Fig. 9 Effect of Miner-Palmgren damage index on reliability

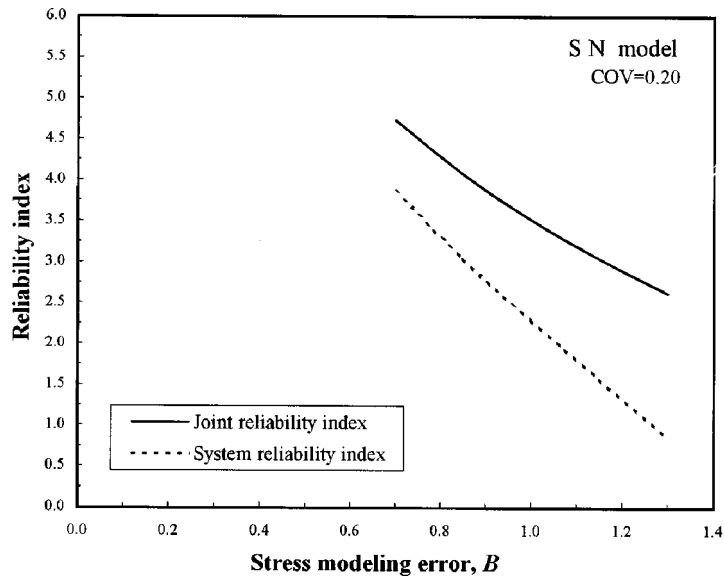


Fig. 10 Effect of stress modeling error, B on reliability

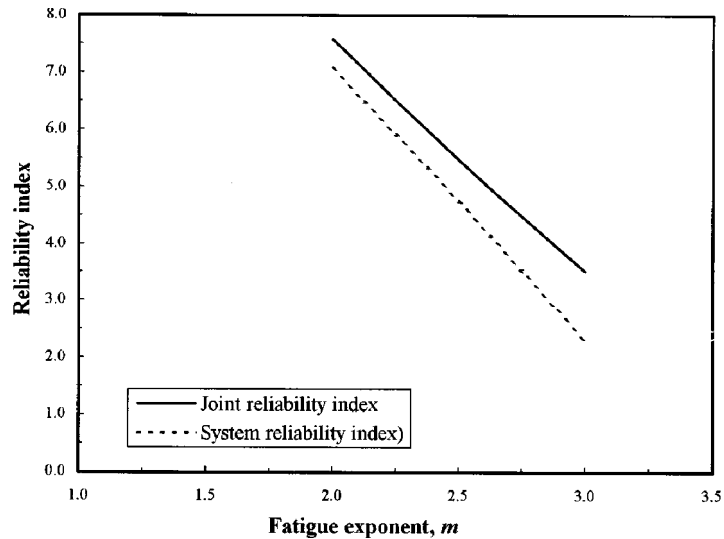


Fig. 11 Effect of fatigue exponent, m on reliability

for fatigue strength coefficient. This indicates that the fatigue strength coefficient influences the reliability more than the Miner-Palmgren damage index ( $\Delta_F$ ). We can also draw the same conclusion from sensitivity analysis (Fig. 2) where, the sensitivity factor of fatigue strength coefficient (A) is more than the Miner-Palmgren damage index ( $\Delta_F$ ). It shows that the fatigue strength coefficient (A) influences the reliability more than the Miner-Palmgren damage index ( $\Delta_F$ ). Fig. 10 shows that as the value of stress modeling error (B) increases, the reliability decreases continuously. This is due to the

fact that  $B$  contributes to the loading part of the limit state function as shown in Fig. 2. Fig. 11 also shows that as the fatigue exponent ( $m$ ) increases, the reliability reduces sharply. It indicates that a great care should be taken in the estimation of fatigue exponent ( $m$ ). The term reliability used in the above discussion is valid for joint reliability as well as the system reliability.

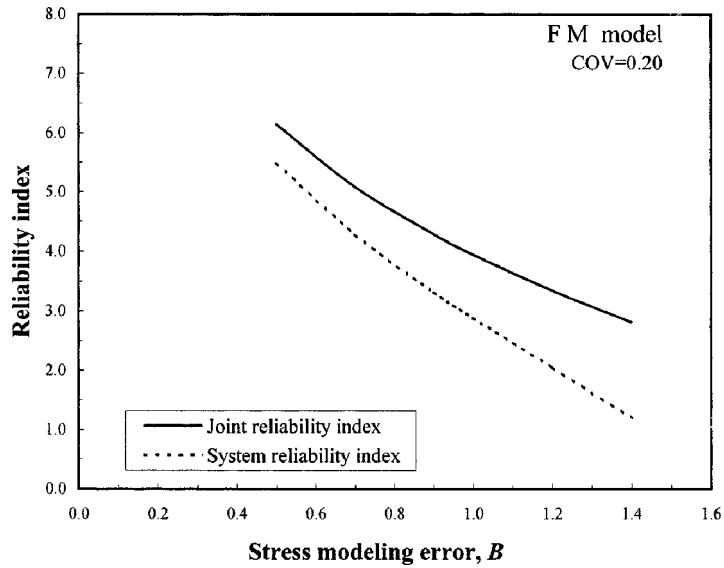


Fig. 12 Effect of stress modeling error,  $B$  on reliability

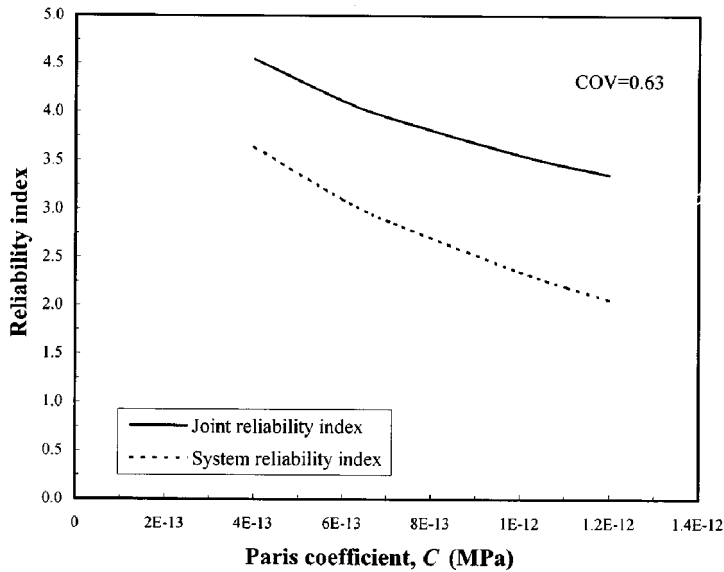


Fig. 13 Effect of Paris coefficient,  $C$  (MPa) on reliability

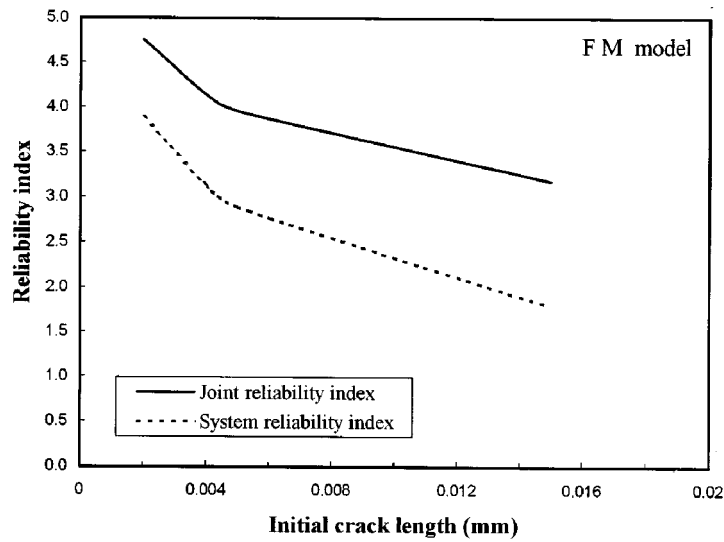


Fig. 14 Effect of initial crack length,  $a_0$  on reliability

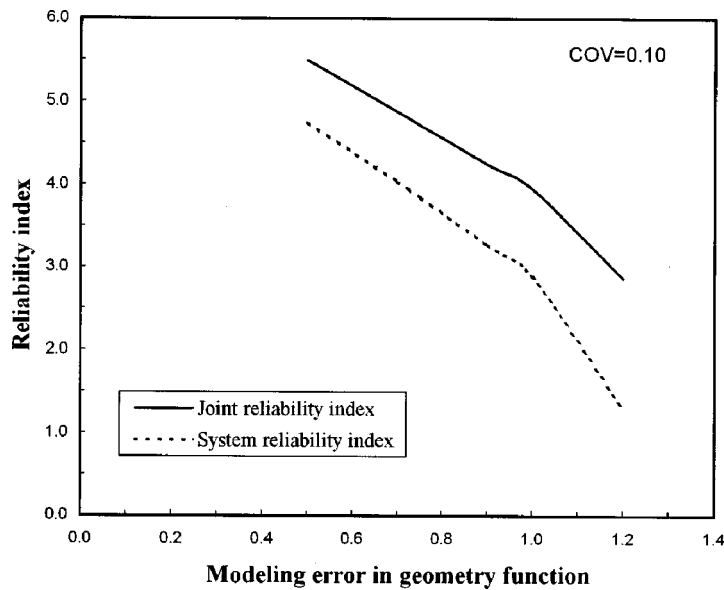


Fig. 15 Effect of modeling error in geometry function on reliability

#### 4.8. Effect of variables in fracture mechanics model

Figs. 12-16 show the effects of various random variables on tether joint and system reliability for given uncertainty. Figs. 12 and 13 show that as the value of stress modeling error ( $B$ ) and Paris coefficient ( $C$ ) increases, the reliability decreases. Fig. 14 shows that as the value of initial crack

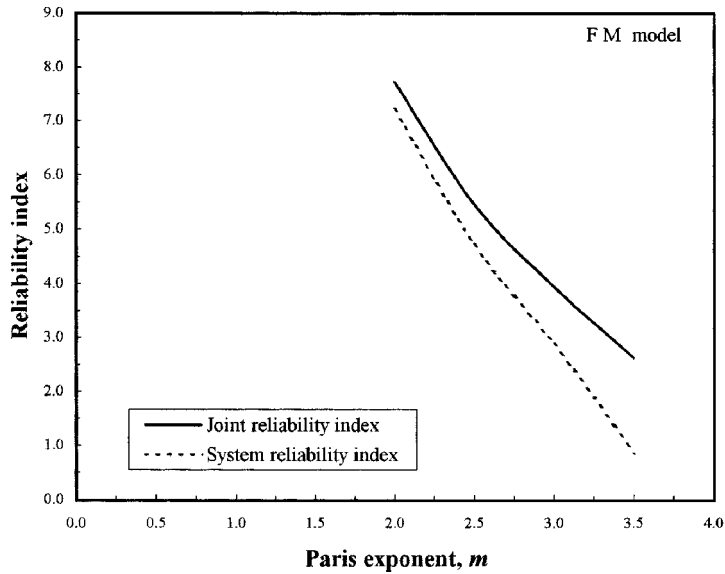


Fig. 16 Effect of Paris exponent,  $m$  on reliability

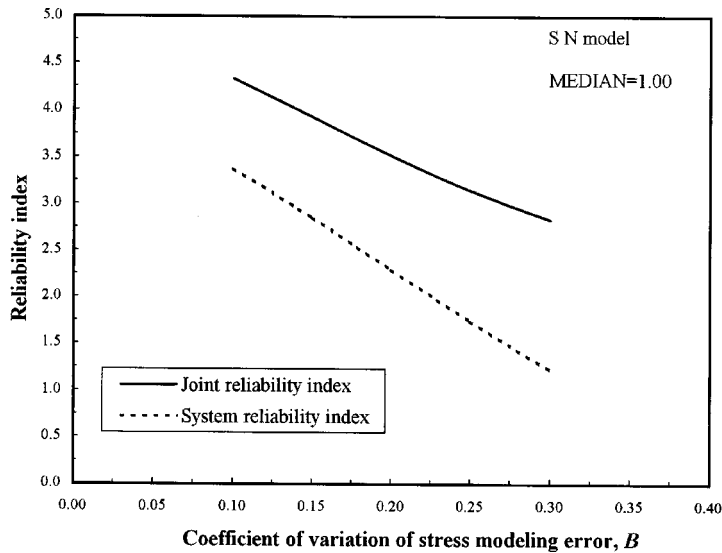


Fig. 17 Effect of uncertainty in stress modeling error,  $B$

length ( $a_0$ ) increases, the reliability decreases sharply up to crack length (i.e., 0.004 mm) then it decreases slowly. Fig. 15 shows that as the value of modeling error ( $\gamma_i$ ) increases, the reliability decreases sharply. This is due to the fact that  $\gamma_i$  contributes to the loading part of the limit state function as shown in Fig.3. Fig. 16 also shows that as the Paris exponent ( $m$ ) increases, the reliability reduces sharply. It indicates that great care should be taken in the estimation of Paris exponent ( $m$ ).

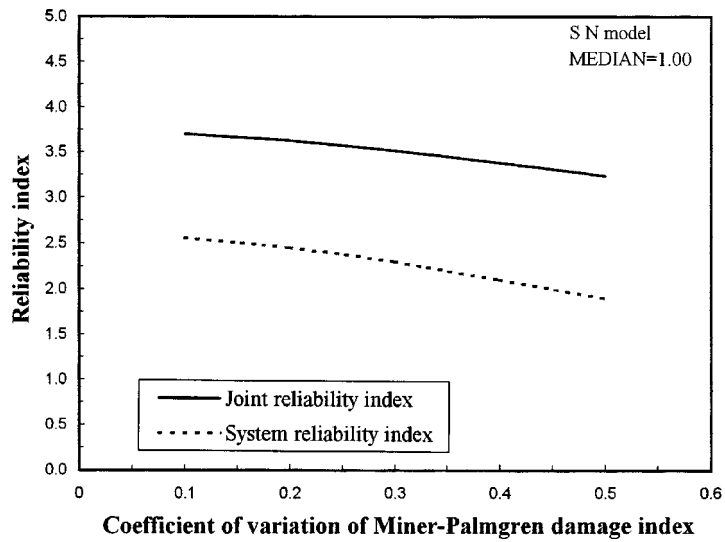


Fig. 18 Effect of uncertainty in Miner-Palmgren damage index

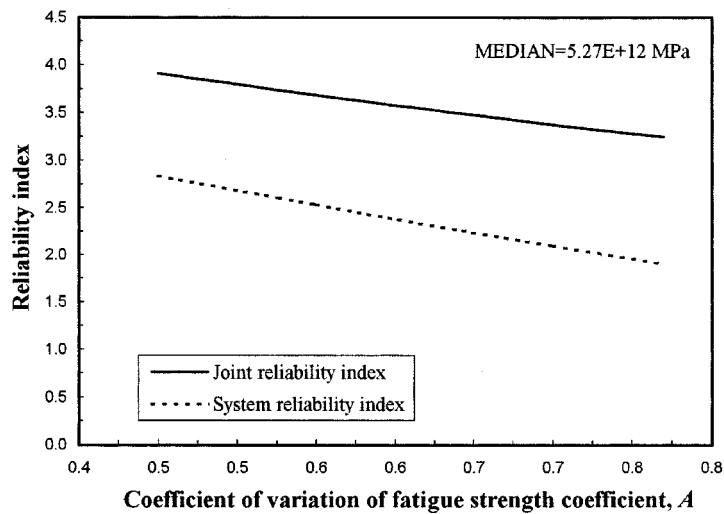


Fig. 19 Effect of uncertainty in fatigue strength coefficient, A

#### 4.9. Effect of uncertainty in S-N model

Figs. 17-19 show that as the uncertainty measured in terms of the coefficient of variation (COV) in stress modeling error ( $B$ ), Miner-Palmgren damage index ( $\Delta_F$ ) and fatigue strength coefficient ( $A$ ) increases, there is corresponding continuous decrease in the reliability index magnitude. This shows that it is not only the mean value that controls the reliability or safety of the tether joint and system but the COV also plays a very significant role in determining the reliability or safety of TLP tethers.

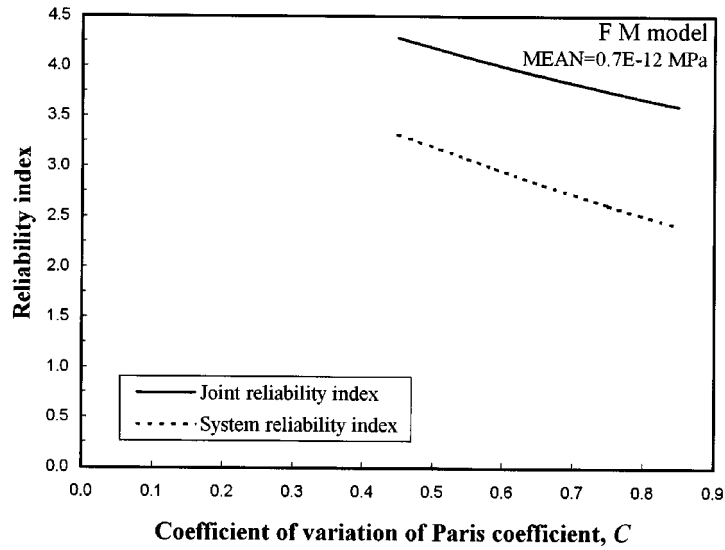


Fig. 20 Effect of uncertainty in Paris coefficient,  $C$

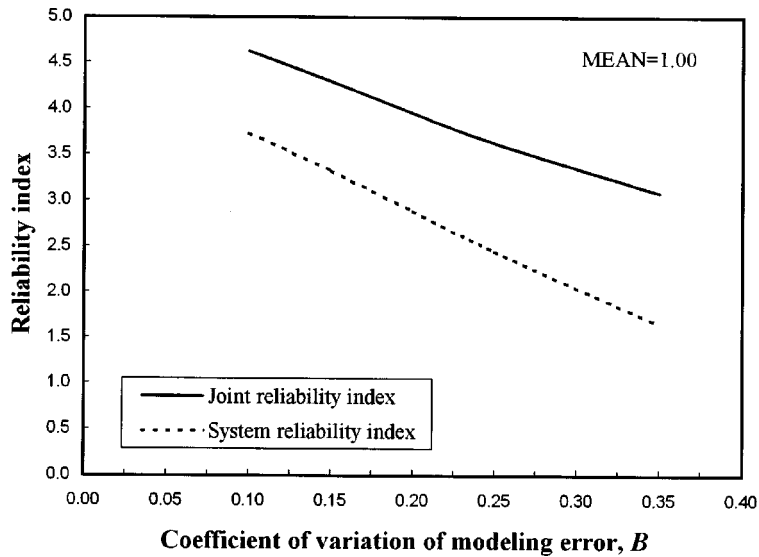


Fig. 21 Effect of uncertainty in stress modeling error,  $B$

#### 4.10. Effect of uncertainty in fracture mechanics model

Figs. 20-22 show that as the uncertainty, measured in terms of the coefficient of variation (COV) in Paris coefficient ( $C$ ), stress modeling error ( $B$ ), and modeling error in geometry ( $\gamma_i$ ) increases, there is corresponding continuous decrease in the reliability index magnitude. This shows again that it is not

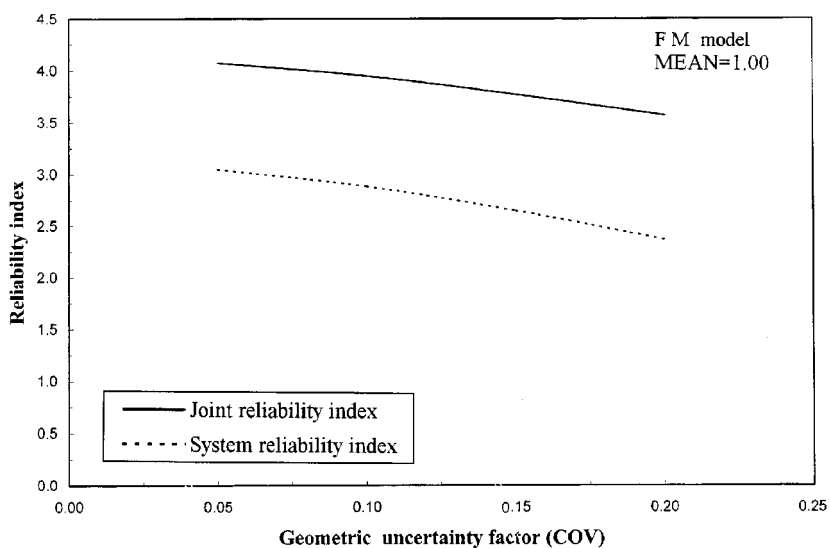


Fig. 22 Effect of uncertainty in geometric uncertainty factor

only the mean value that controls the reliability or safety of tether joint and system but the COV also plays a very significant role in determining the reliability.

## 6. Conclusions

The present paper presents a detailed methodology for the fatigue reliability analysis of welded joints. The methodology presented is applied to TLP tether system, however, it is quite general and can be applied to varieties of steel structure problem which has fatigue sensitive joints. To study the influence of various random variables on tether reliability sensitivity analysis has been carried out. The results of this analysis are found to be very important design tool. Some parametric studies have also been included to obtain the results of field interest.

## References

- Chao, R. and Ayyub, B. M. (1997), "Reliability and uncertainty evaluation for longitudinal bending of hull girders of surface ships", *J. Ship Research*, **41**(1), 57-68.
- Kjerengtroen, L. and Wirsching, H. (1984), "Structural reliability analysis of series system", *J. Struct. Eng.*, ASCE, **110**(7), 1495-1511.
- Kung and Wirsching (1992), "Fatigue and fracture reliability and maintainability of TLP tendons", *OMAE, Safety and Reliability*, ASME, vol. II, 15-21.
- Wirsching, P. H. and Chen, Y. N. (1987), "Fatigue design criteria for TLP tendons", *J. Struct. Eng.*, ASCE, **113**(7), 1398-1414.
- Paris, P. C. (1964), The fracture mechanics approach to fatigue. In: Burke JJ, Reed NL, Weiss V, editors. *Fatigue and interdisciplinary approach*. Syracuse, New York: Syracuse University Press, 107-132.
- Madsen, H. O., Krenk, S. and Lind, N. C. (1986), *Methods of Structural Safety*. Prentice-Hall, Eaglewood Cliffs, NJ.

- Siddiqui, N. A. and Ahmad, S. (1999), "Fatigue reliability analysis of TLP tethers under random wave and wind loading", *Proceedings of the 11<sup>th</sup> ISME conference on Mechanical Engineering*, IIT Delhi, 208-215.
- Siddiqui, N. A. and Ahmad, S. (2000), "Reliability analysis against progressive failure of TLP tethers in extreme tension," *Reliability Engineering and System Safety (RESS)*, **68**(3), 195-205.
- Siddiqui, N. A. and Ahmad, S. (2001), "Fatigue and fracture reliability of TLP tethers under random loading", *Marine Structures*, **14**(3), 331-352.
- Tornøe, T. Y. and Wirsching, P. H. (1991), "Fatigue and fracture reliability and maintainability process", *J. Struct. Eng.*, ASCE, **117**(12), 3804-3822.
- CC